Comparative analysis of exosomal miRNAs derived from lipopolysaccharide and polyinosinic-polycytidylic acid-stimulated chicken macrophage cell line

Yeojin Hong,* Thi Hao Vu,* Sooyeon Lee,* Jubi Heo,* Suyeon Kang,* Hyun S. Lillehoj,† and Yeong Ho Hong *,1

*Department of Animal Science and Technology, Chung-Ang University, Anseong 17546, Republic of Korea; and †Animal Biosciences and Biotechnology Laboratory, Agricultural Research Services, United States Department of Agriculture, Beltsville, MD 20705, USA

ABSTRACT Exosomes play important roles in cellular communication by delivering exosomal proteins and nucleic acid molecules to cells. In particular, exosomal miRNAs can modulate various biological processes in recipient cells by repressing target gene expression. In this study, to identify the composition of exosomal miRNAs and their regulatory mechanisms against bacterial and viral infections, profiles of exosomal miRNAs from lipopolysaccharide (**LPS**) and polyinosinic-polycytidylic acid (**poly(I:C)**)-stimulated chicken macrophage cell line (HD11) were analyzed by small RNA sequencing. Exosomes were purified after stimulation with LPS (1 μg/mL) and poly(I:C) (50 μg/mL) for 24 h. Then, exosomal RNA were analyzed for small RNA sequencing using the HiSeq 2500 System. Thirty six differentially expressed miRNAs (**DE miRNAs**) were obtained by comparing LPS-stimulated exosomes (**LPS-EXO**) and unstimulated exosomes (**CTRL-EXO**), 42 DE miRNAs in poly(I:C)-stimulated exosomes (**POLY-EXO**) and CTRL-EXO, and 45 DE miRNAs in LPS-EXO and POLY-EXO. Target genes of DE miRNAs were predicted using miRDB and TargetScan. KEGG pathway analysis showed that most of the target genes were related to mitogen-activated protein kinase and Wnt signaling pathways. Moreover, results of qRT-PCR for miRNAs (gga-miR-142-3p, gga-miR-19a-3p, gga-miR-21-3p, gga-miR-301a-3p, gga-miR-338-3p, and gga-miR-3523) were consistent with the sequencing results. This study will provide knowledge about immuno-regulatory mechanisms of exosomal miRNAs derived from macrophages against pathological insults such as bacterial and viral infections.

Key words: exosomes, LPS, poly(I:C), miRNAs, chicken, macrophages

2022 Poultry Science 101:102141
https://doi.org/10.1016/j.psj.2022.102141

INTRODUCTION

Macrophages defend the host against pathogen infections by regulating the innate and adaptive immune systems (Billack, 2006). In particular, macrophages recognize foreign stimuli using receptors such as toll-like receptors and other pattern recognition receptors, by detecting pathogen-associated molecular patterns of pathogens (Reimer et al., 2008). Activated macrophages kill invading pathogens by phagocytosis and stimulate the immune system through various pathways (Aderem and Underhill, 1999; Koh and DiPietro, 2011).

Lipopolysaccharide (**LPS**), a structural component of gram-negative bacteria, is detected by TLR4. In addition, polyinosinic-polycytidylic acid (**poly(I:C)**), a synthetic double-stranded RNA (**dsRNA**) generated during the replication of viruses, is detected by TLR3, cytosolic RNA helicases retinoic acid-inducible protein I (absent in chicken), and melanoma differentiation-associated protein 5 (**MDA-5**) (Thompson et al., 2011). Upon LPS recognition, the signal is transmitted to the nucleus by activating nuclear factor kappa-light-chain-enhancer of activated B cells (**NF-κB**) and transcription of proinflammatory cytokines is induced. When poly(I:C) is recognized by their receptors, the signal stimulates activation of interferon regulatory factor3/7 and NF-κB by inducing transcription of type I interferons (Kim and Zhou, 2015).

Extracellular vesicles (**EVs**) are cell membrane-derived vesicles with a diverse diameter of 30 to 1,000 nm (Tkach and Théry, 2016). EVs can be divided into 3 classes according to the method of secretion from cells— microvesicles, exosomes, and apoptotic bodies (Zhang et al., 2015; Chen et al., 2018). Exosomes involve

Received October 5, 2021.
Accepted August 21, 2022.

[1]Corresponding author: yhong@cau.ac.kr

multiple components, including membrane proteins, cytoskeletal proteins, MVB-making proteins, signaling proteins, enzymes, mRNAs, microRNAs (**miRNAs**), other non-coding RNAs, and DNA (Mathivanan et al., 2010; Gross et al., 2012). In particular, exosomal miRNAs, the small non-coding RNAs, can modulate various biological processes by repressing the translation of target mRNAs in recipient cells (Tkach et al., 2016; Boulanger et al., 2017). Therefore, those derived from immune cells can be transferred to recipient cells where they inhibit the expression of target genes by regulating biological responses such as induction of anti-/pro-inflammation, wound healing, and tumor (Montecalvo et al., 2012; Ti et al., 2015; Dalvi et al., 2017; Yin et al., 2019; Kalluri and LeBleu, 2020).

Macrophages are essential immune cells for phagocytosis, wound healing, antigen presentation, and cytokine production (Aderem and Underhill, 1999; Koh and DiPietro, 2011). Macrophages defend the host against bacterial and viral infections. LPS, a structural component of gram-negative bacteria, and poly(I:C), a synthetic viral-like dsRNA, can simulate bacterial and viral infection in macrophages, respectively. Our previous studies have shown that LPS and poly(I:C)-stimulated exosomes modulate the immune response of chicken macrophages and T cells (Hong et al., 2021a, b). However, exosomal contents of LPS- and poly(I:C)-stimulated cells have not been studied yet. Therefore, we conducted exosomal small RNA sequencing and analyzed expression profiles of exosomal miRNAs derived from LPS- and poly(I:C)-stimulated chicken macrophage cell line (HD11) to determine immune response induced by LPS and poly(I:C) is reflected in exosomal miRNA composition and to identify regulatory mechanisms of miRNAs.

MATERIALS AND METHODS

Cell line Culture

The chicken macrophage cell line HD11 (Klasing and Peng, 1987) was maintained in complete Roswell Park Memorial Institute (**RPMI**) 1640 medium (Thermo Fisher Scientific, Waltham, MA) containing 100 IU/mL penicillin, 100 mg/mL streptomycin, and 10% heat-inactivated fetal bovine serum (Thermo Fisher Scientific) in a humidified 5% CO_2 atmosphere at 41°C. For exosome purification, HD11cells (1.0×10^7) were seeded in eight 100-mm cell culture dishes (SPL Life Sciences, Pocheon, Korea) with complete RPMI 1640 medium. The next day, the medium was replaced with fresh exosome-depleted RPMI 1640 medium containing 100 IU/mL penicillin, 100 mg/mL streptomycin, and 10% exosome-depleted fetal bovine serum (#EXO-FBSHI-250A-1; System Bioscience, Palo Alto, CA) with or without 1 μg/mL LPS from *Escherichia coli* O127:B8 (#L4516; Sigma-Aldrich, St. Louis, MO) and 50 μg/mL poly(I:C) (#P1530; Sigma-Aldrich) and incubated for 24 h. Then, the cell culture supernatant was collected for exosome purification.

Exosome Purification

A total of 80 mL of cell culture supernatant was collected to purify exosomes with ExoQuick-TC (#EXOTC50A-1; System Bioscience) following the manufacturer's protocol. Cell culture supernatants were centrifuged at 3,000 × *g* for 15 min. Supernatants were then transferred, mixed with 16 mL of ExoQuick-TC by inverting, and incubated overnight at 4°C. The mixture was subsequently centrifuged at 1,500 × *g* for 30 min, following which, exosomes were resuspended in 600 μL of phosphate-buffered saline (pH 7.4). The concentration of purified exosomes was measured using the Pierce bicinchoninic acid protein assay kit (Thermo Fisher Scientific) according to the manufacturer's instructions. For the characterization of exosomes, particle size was measured using a nanoparticle analyzer (SZ-100; Horiba, Kyoto, Japan). Furthermore, a western blot assay was performed using CD9 (#13174, Cell Signaling Technology, Danvers, MA) and CD81 (#56039, Cell Signaling Technology) antibodies according to previously described methods (Hong et al., 2020).

Exosomal RNA Extraction and Small RNA Sequencing

Exosomal RNA was extracted using the miRNeasy Serum/Plasma Kit (Qiagen, Hilden, Germany) according to the manufacturer's instructions. Library construction and small RNA sequencing were conducted for exosomes from unstimulated HD11 (**CTRL-EXO**), LPS-stimulated HD11 (**LPS-EXO**), and poly(I:C)-stimulated HD11 (**POLY-EXO**). The library was constructed using the SMARTer smRNA-Seq Kit for Illumina (TAKARA Bio Inc., Otsu, Shiga, Japan) according to the manufacturer's instructions. Next, small RNA sequencing was conducted by Macrogen (Seoul, Republic of Korea) using a HiSeq 2500 System (Illumina Inc., San Diego, CA).

Bioinformatics Analysis

After sequencing, raw sequence reads were filtered based on quality using FastQC v0.11.7 (http://www.bioinformatics.babraham.ac.uk/projects/fastqc/). Adapter sequences were additionally trimmed from raw sequence reads using Cutadapt 2.8 (https://cutadapt.readthedocs.org/en/stable/). Both trimmed reads and non-adapter reads analyzed long targets (≥ 50bp), and processed reads were then gathered to form a unique cluster. Unique clustered reads were sequentially aligned to the reference genome, miRBase v22.1 (http://www.mirbase.org/), and non-coding RNA database, RNAcentral 14.0 (https://rnacentral.org/) to classify known miRNAs and other types of RNA such as tRNA, snRNA, and snoRNA. Genome mapping was performed using Bowtie v1.1.2 (http://bowtie-bio.sourceforge.net/index.shtml) and RSEM version v1.3.1, STAR 2.6.0c (http://deweylab.github.io/RSEM/). Known/novel miRNAs

predicted by miRDeep2 v2.0.0.8 (https://www.mdc-berlin.de/content/mirdeep2-documentation) and other miRNAs matching RNAcentral were aligned using Bowtie (target smRNA, <50 nt) and HISAT2 version 2.1.0, Bowtie2 2.3.4.1 (https://daehwankimlab.github.io/hisat2/) (target smRNA, ≥50nt). Read counts for each miRNA were extracted from mapped miRNAs to determine the abundance of each miRNA. For differentially expressed miRNA (**DE miRNA**) analysis, read counts of mature miRNAs obtained from miRDeep 2 were used as the original raw data. During data pre-processing, low-quality miRNAs were filtered, and TMM normalization was performed. Statistical analysis of DE miRNAs was performed using fold change and exact Test using edge R (**empirical analysis of digital gene expression data in R**). Significant results were selected on the conditions of |fold-change|≥2 & exact Test raw P-value < 0.05. For significant DE miRNAs, hierarchical clustering analysis was performed to group similar samples and mature miRNAs. Target genes of DE miRNAs were predicted using miRDB (http://www.mirdb.org/) and TargetScan (http://www.targetscan.org/vert_72/). Target genes with a target score over 80 were selected in miRDB, and genes with conserved sites in TargetScan were selected. Gene ontology (**GO**) functional enrichment analysis of target genes was performed using gProfiler (http://biit.cs.ut.ee/gprofiler/gost).

miRNA Primer Design

Quantitative real-time PCR (**qRT-PCR**) for miRNAs required a forward primer to be designed for individual miRNAs and a universal reverse primer provided with the miScript SYBR Green PCR Kit (Qiagen). All known chicken miRNA sequences were obtained from miRBase (http://microrna.sanger.ac.uk/sequences/ftp.shtml). Oligonucleotide primers for these miRNAs were designed using full-length mature miRNA sequences. Primers were synthesized by Genotech (Daejeon, South Korea; Table 1).

miRNA Expression Analysis by qRT-PCR

cDNA synthesis was performed using the miScript II RT Kit (Qiagen) according to previously described methods (Hong et al., 2021c). The synthesized cDNA was used as a template for qRT-PCR. The miScript SYBR Green PCR Kit (Qiagen) was used to determine miRNA expression in the CFX Connect Real-Time PCR Detection System (Bio-Rad, Hercules, CA) according to the manufacturer's protocol. In brief, for 25 μL of reaction mix, the following components were added: 12.5 μL of 2 × QuantiTect SYBR Green PCR Master Mix, 2.5 μL of 10 μM forward primer, 2.5 μL of 10 × universal primer, 2.5 μL of template cDNA, and RNase-free water up to 25 μL. The cycling conditions were as follows: 95°C for 15 min to activate the initial step, followed by 40 cycles of 94°C for 15 s, 55°C for 30 s, and 70°C for 30 s. Gene expression was calculated using the $2^{-\Delta\Delta Ct}$ method after normalization with U1A (Livak and Schmittgen, 2001). All qRT-PCR analyses were performed in triplicates.

Table 1. Sequences of primers for qRT-PCR analysis.

miRNAs	Sequences (5′- 3′)
U1A	CTGCATAATTTGTGGTAGTGG
gga-miR-19a-3p	TGTGCAAATCTATGCAAAACTGA
gga-miR-21-3p	CAACAACAGTCGGTAGGCTGTC
gga-miR-301a-3p	CAGTGCAATAATATTGTCAAAGCAT
gga-miR-338-3p	TCCAGCATCAGTGATTTTGTTGA
gga-miR-3523	CCGCGCAGTGCCTCGTCCTCGA

Statistical Analysis

Statistical analysis was performed using SPSS software (version 26.0; IBM, Chicago, IL). Data are expressed as the mean ± SEM. Statistical comparisons were performed using one-way ANOVA and Tukey's multiple comparison test, and the level of statistical significance was set at $P < 0.05$.

RESULTS

Characterization of Exosomes

Exosomes from LPS- and poly(I:C)-stimulated HD11 and non-stimulated HD11 were purified and characterized by particle size and exosomal biomarkers (Figure S1). The size range of exosome was 72.87 to 279.04 nm for CTRL-EXO, 93.02 to 315.27 nm for LPS-EXO, and 82.33 to 315.27 nm for POLY-EXO. The average size of exosomes was 132 nm for CTRL-EXO, 169 nm for LPS-EXO, and 159.9 nm for POLY-EXO (Figure S1A). Exosomal markers of CD9 and CD81 were detected by western blotting in CTRL-EXO, LPS-EXO, and POLY-EXO (Figure S1B).

Statistical Assessment of Small RNA Sequencing

In CTRL-EXO, 56,954,938 reads were produced, and the total read bases were 2.9 Gbp, while those of LPS-EXO and POLY-EXO were 46,637,883 reads and 2.4 Gbp and 45,066,267 reads and 2.3 Gbp, respectively (Table 2). GC contents of CTRL-EXO, LPS-EXO, and POLY-EXO were 36.74, 39.28, and 36.49%, respectively, and the corresponding ratio of bases with a Phred quality score ≥30 (Q30) were 89.4, 87.06, and 80.42%. Table 3 shows the number of mapped reads to the

Table 2. Raw data statistics (raw FASTQ statistics).

Sample	Total bases	Read count	GC (%)	Q20 (%)	Q30 (%)
CTRL-EXO	2,904,701,838	56,954,938	36.74	93.78	89.4
LPS-EXO	2,378,532,033	46,637,883	39.28	92.31	87.06
POLY-EXO	2,298,379,617	45,066,267	36.49	86.8	80.42

Total bases (= Total reads × Read length) indicate the total number of bases sequenced.

Q20 (%) and Q30 (%) are ratios of bases that have phred quality score greater than or equal to 20 and 30, respectively.

Table 3. Mapped reads to miRBase precursor.

Sample	Processed reads	Mapped reads	Known miRNA in Sample	Known miRNA in Species (miRBase v22.1)
CTRL-EXO	34,634,118	207,112 (0.6%)	361	1,235
LPS-EXO	23,012,701	90,736 (0.39%)	297	1,235
POLY-EXO	20,519,518	10,440 (0.05%)	168	1,235

Processed reads indicate reads which were trimmed and removed unwanted sources from them.

miRBase precursor and the number of known miRNAs with read counts greater than 1 for each sample. In CTRL-EXO, among 34,634,118 processed reads, 207,112 (0.6%) reads mapped to the miRBase precursor, and 361 known miRNAs were detected, while those in LPS-EXO and POLY-EXO corresponded to 23,012,701 processed reads, 90,736 (0.39%) reads, 297 known miRNAs and 20,519,518 processed reads, 10,440 (0.05%) reads mapped, and 168 known mi RNAs.

Analysis of Differentially Expressed miRNAs Between CTRL, LPS, and POLY-EXOs

DE miRNAs were analyzed in 3 comparison groups: LPS-EXO vs. CTRL-EXO, POLY-EXO vs. CTRL-EXO, and LPS-EXO vs. POLY-EXO. In the LPS-EXO vs. CTRL-EXO comparison, a total of 36 DE miRNAs were found, and 23 miRNAs were upregulated and 13 miRNAs were downregulated in LPS-EXOs compared with those in CTRL-EXO (Figure 1). In POLY-EXO vs. CTRL-EXO comparison, 42 DE miRNAs were detected, and 28 miRNAs were upregulated and 14 miRNAs were downregulated in POLY-EXO compared with those in CTRL-EXO. In the LPS-EXO vs. POLY-EXO comparison, a total of 45 DE miRNAs were found, and 19 miRNAs were upregulated and 26 miRNAs were downregulated in LPS-EXO compared with those in POLY-EXO. TableS1 shows the fold change in DE miRNAs and read counts. Among 36 DE miRNAs in LPS-EXO vs. CTRL-EXO comparison, the expression level of gga-miR-16c-5p was the highest, with a fold change of 19.51, and the expression level of

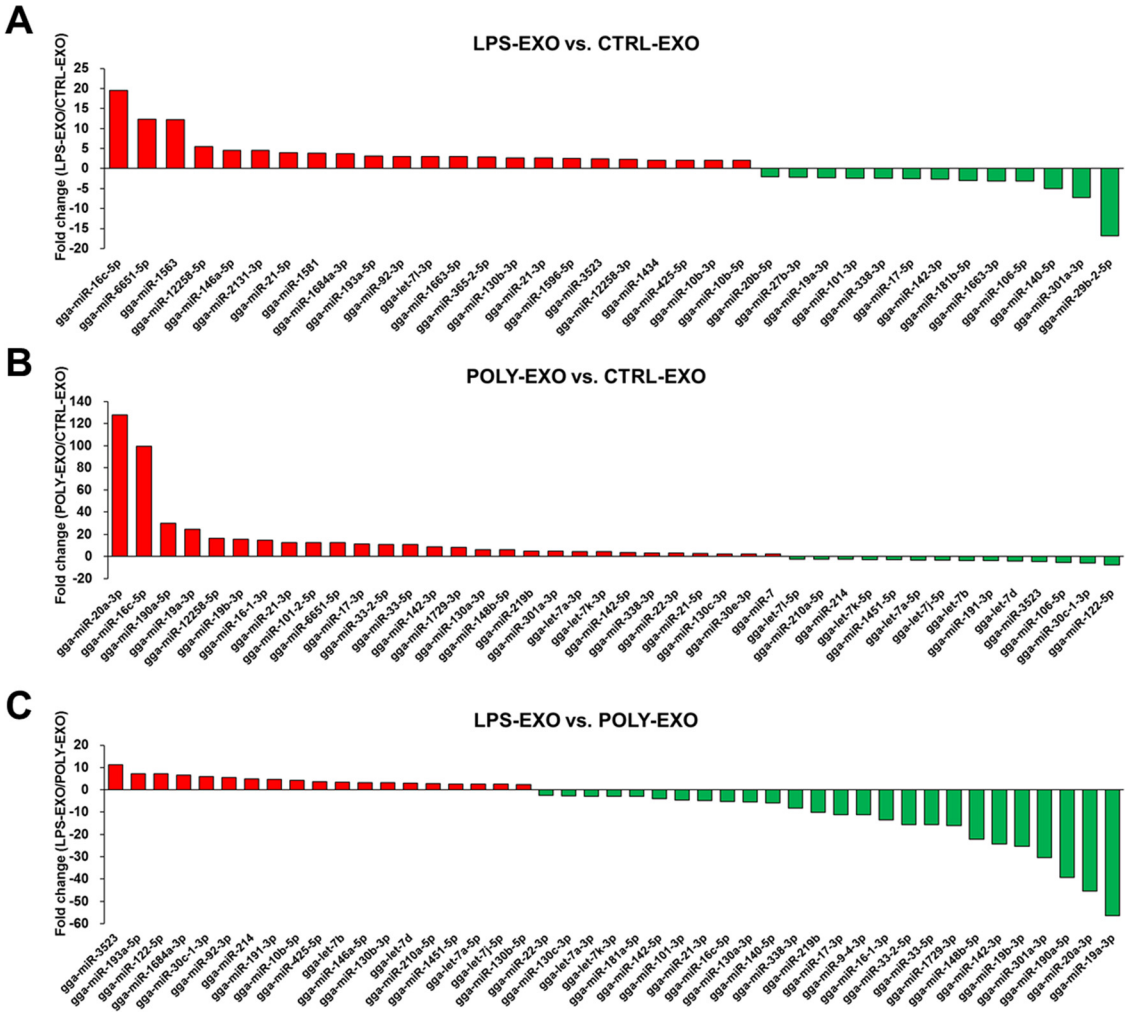

Figure 1. Fold-change of differentially expressed miRNAs of (A) lipopolysaccharide-stimulated exosomes (LPS-EXO) vs. unstimulated HD11 (CTRL-EXO), (B) poly(I:C)-stimulated exosomes (POLY-EXO) vs. CTRL-EXO, and (C) LPS-EXO vs. POLY-EXO. Significant differentially expressed miRNAs were selected on conditions of $|FC| \geq 2$ and exact Test raw P-value < 0.05.

gga-miR-29b-2-5p was the lowest, with a fold change of −16.77 in LPS-EXO. Among 42 DE miRNAs in POLY-EXO vs. CTRL-EXO comparison, expression of gga-miR-20a-3p was the highest, with a fold change of 127.91, and the expression level of gga-miR-122-5p was the lowest, with a fold change −7.62 in POLY-EXO. Among the 45 DE miRNAs in LPS-EXO vs. POLY-EXO comparison, the expression level of gga-miR-3523 was the highest, with a fold change of 11.21, and the expression level of gga-miR-19a-3p was the lowest, with a fold change of −56.45 in LPS-EXO. In the volcano plot, $\log_2$ fold change and *P*-values obtained from the comparison between the 2 groups were plotted (Figure 2). We further compared 70 miRNAs among the 3 samples and performed heat map and hierarchical clustering analysis, as shown in Figure 3. miRNA expression pattern of CTRL-EXO was similar to LPS-EXO than POLY-EXO. Moreover, although the expression pattern of miRNAs in LPS-EXO and POLY-EXO had some similarities, most miRNAs expressions were opposite. Figure 4 shows the Venn diagram of DE miRNAs in the 3 comparisons. Seven miRNAs (gga-miR-338-3p, gga-miR-142-3p, gga-miR-19a-3p, gga-miR-16c-5p, gga-miR-3523, gga-miR-21-3p, and gga-miR-301a-3p) were found to be overlapping DE miRNAs in the 3 comparisons. Moreover, 4 miRNAs (gga-miR-6651-5p, gga-miR-12258-5p, gga-miR-21, and gga-miR-106-5p) were common DE miRNAs only in LPS-EXO vs. CTRL-EXO and POLY-EXO vs. CTRL-EXO comparisons. 9 miRNAs (gga-miR-10b-5p, gga-miR-130b-3p, gga-miR-146a-5p, gga-miR-92-3p, gga-miR-1684a-3p, gga-miR-193a-5p, gga-miR-101-3p, gga-miR-425-5p, gga-miR-140-5p) were found as common DE miRNAs only in LPS-EXO vs. CTRL-EXO and LPS-EXO vs. POLY-EXO comparisons. 26 miRNAs (gga-miR-214, gga-miR-1451-5p, gga-miR-30c-1-3p, gga-miR-130a-3p, gga-miR-19b-3p, gga-miR-20a-3p, gga-miR-210a-5p, gga-miR-148b-5p, gga-miR-190a-5p, gga-miR-17-3p, gga-miR-122-5p, gga-miR-1729-3p, gga-let-7k-3p, gga-let-7d, gga-miR-22-3p, gga-miR-142-5p, gga-miR-33-2-5p, gga-let-7b, gga-miR-16-1-3p, gga-miR-33-5p, gga-miR-191-3p, gga-let-7a-5p, gga-miR-219b, gga-miR-130c-3p, gga-let-7a-3p, and gga-let-7j-5p) were

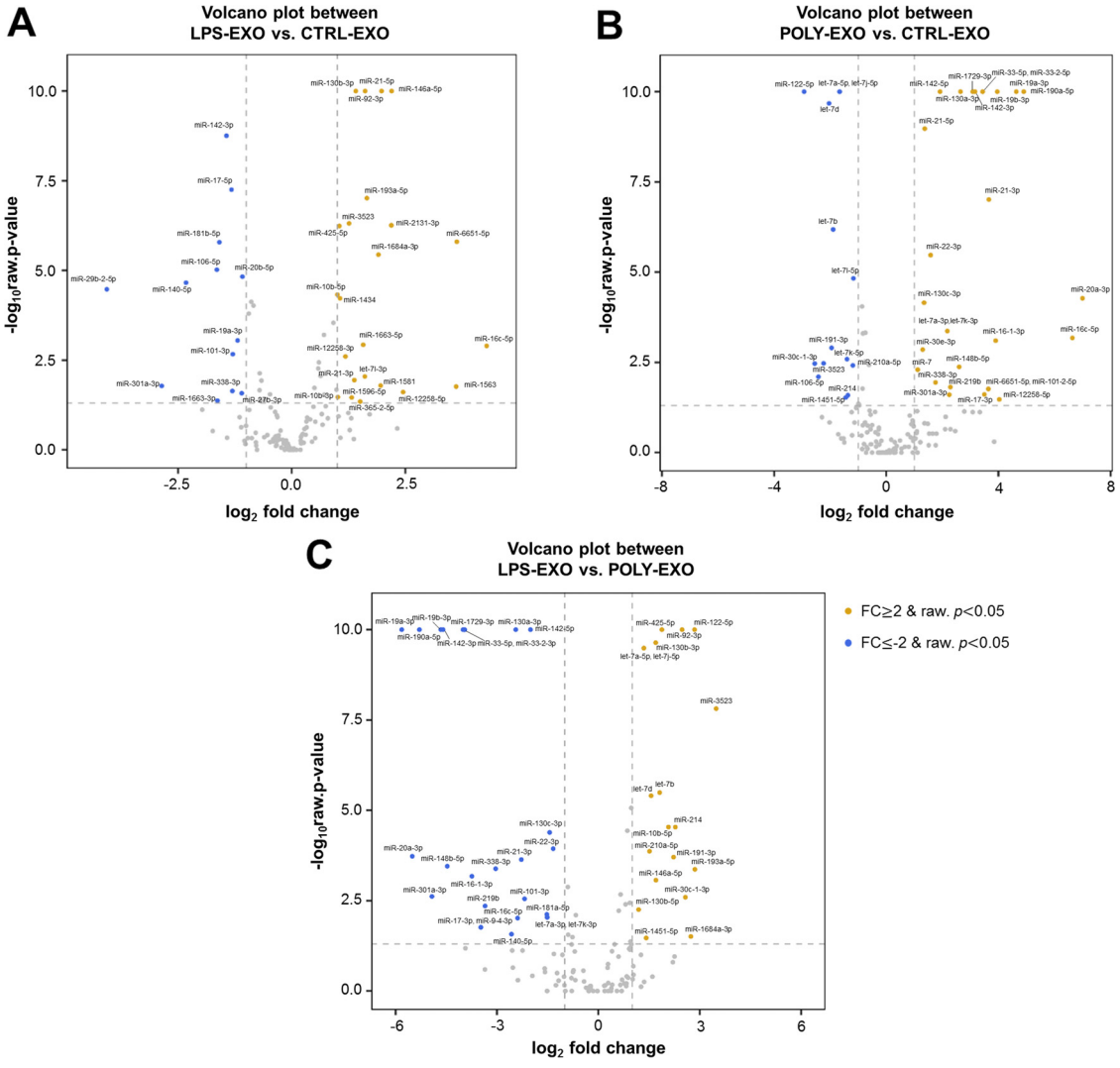

Figure 2. Volcano plot of differentially expressed miRNAs of (A) lipopolysaccharide-stimulated exosomes (LPS-EXO) vs. unstimulated HD11 (CTRL-EXO), (B) poly(I:C)-stimulated exosomes (POLY-EXO) vs. CTRL-EXO, and (C) LPS-EXO vs. POLY-EXO. The vertical lines correspond to 2-fold up and down, respectively, and the horizontal line represents a *P*-value of 0.05. X-axis, $\log_2$ fold-change; Y-axis, $-\log_{10}$ *P*-value. Yellow dots indicate FC ≥ 2 and raw *P*-value < 0.05; blue dot indicate FC ≤−2 and raw *P*-value < 0.05.

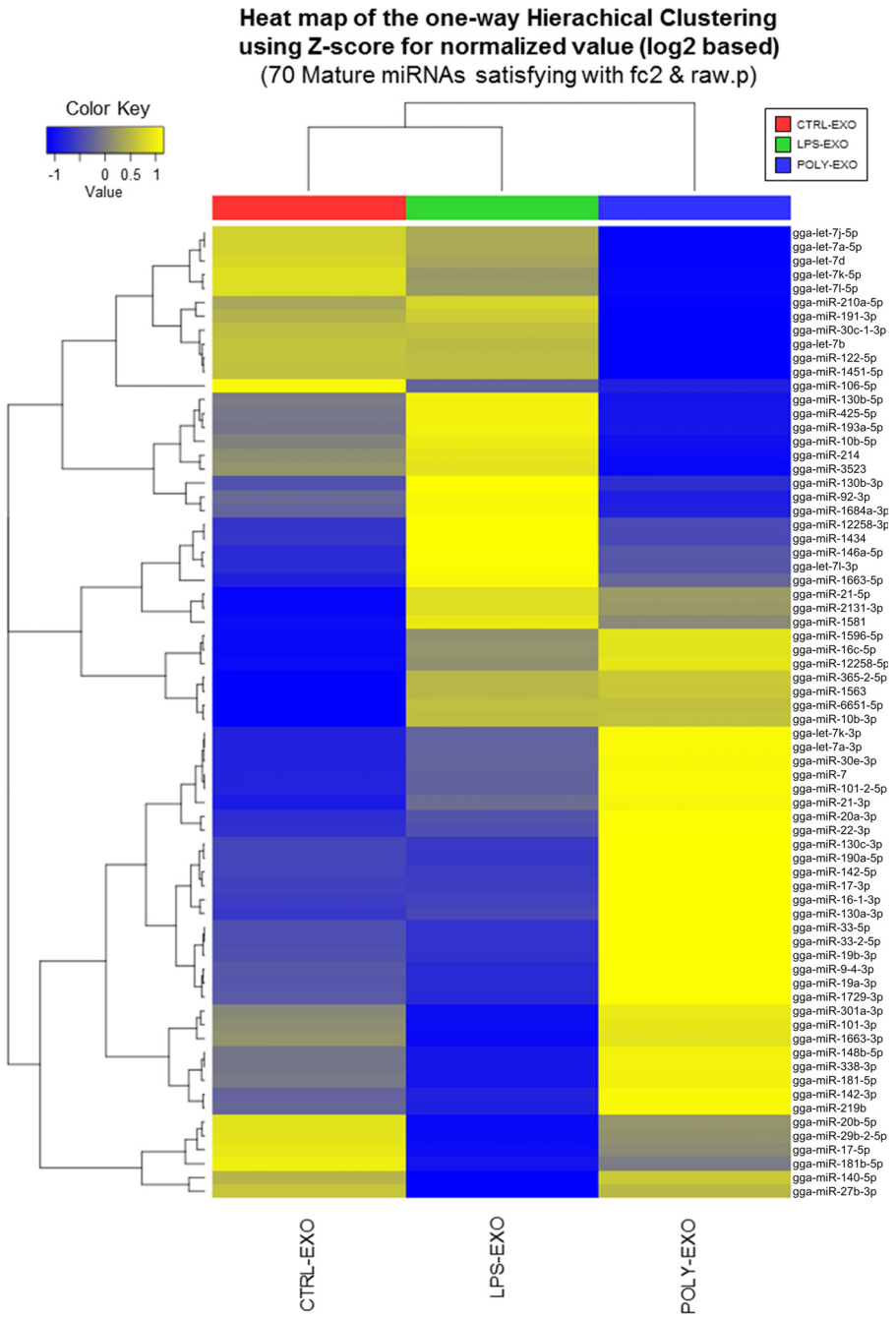

Figure 3. Heatmap and hierarchical clustering analysis of 70 differentially expressed miRNAs using R program. This analysis was conducted using the Euclidean method and complete linkage. The red color box indicates unstimulated HD11 (CTRL-EXO), the green color box indicates lipopolysaccharide-stimulated exosomes (LPS-EXO), and the blue color box indicates poly(I:C)-stimulated exosomes (POLY-EXO). Z-score is the estimated coefficient of variation divided by its standard error.

overlapping DE miRNAs only in POLY-EXO vs. CTRL-EXO and LPS-EXO vs. POLY-EXO comparisons.

Target Genes Prediction

For each comparison, prediction of target genes of DE miRNAs was performed using miRDB and TargetScan. Target genes with a target score over 80 were selected in miRDB, and genes with conserved sites in TargetScan were selected. A Venn diagram of the predicted target genes by miRDB and TargetScan is presented in Figure 5. In the LPS-EXO and CTRL-EXO comparisons, 3,743 target genes were predicted by miRDB, 5,416 target genes were predicted by TargetScan, and 2,139 genes overlapped (Figure 5A). In the POLY-EXO and CTRL-EXO comparisons, 3,805 target genes were predicted by miRDB, 6,034 target genes were predicted by TargetScan, and 2,274 genes overlapped (Figure 5B). In the LPS-EXO and POLY-EXO comparisons, 4,095 genes were predicted as target genes by miRDB and 6,072 genes were predicted as target genes by TargetScan, and 2,420 genes overlapped (Figure 5C).

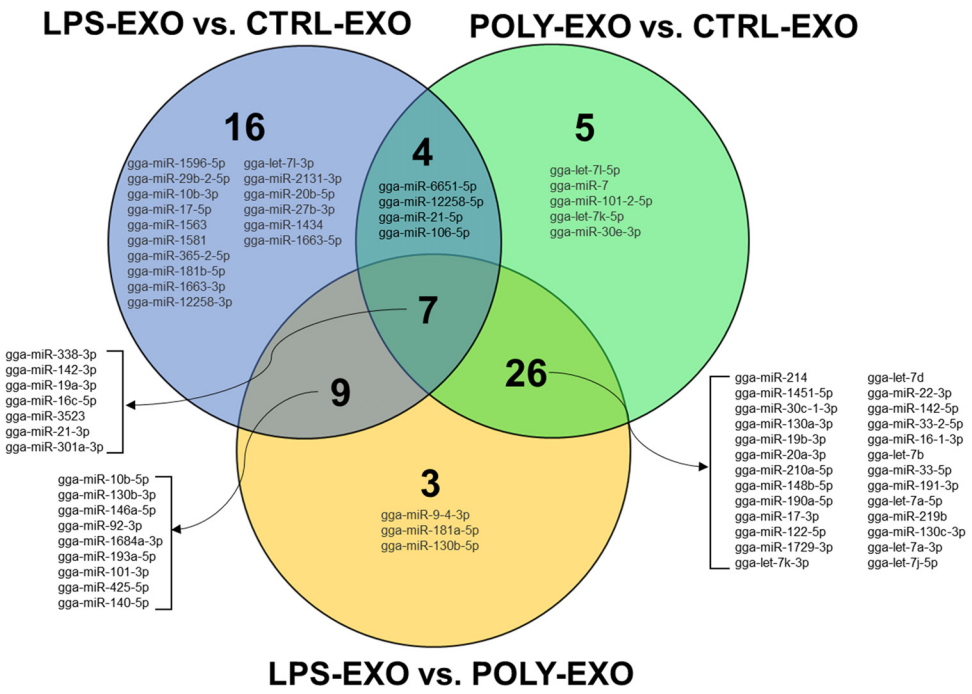

Figure 4. Venn diagram for overlapping differentially expressed miRNAs in three comparisons. The numbers indicate miRNA counts in the indicated area.

GO and KEGG Pathway Analysis

For GO and KEGG pathway analyses, overlapping target genes between miRDB and TargetScan were used. In GO analysis, 2,139 target genes from LPS-EXO vs. CTRL-EXO were classified into 60 GO terms for molecular functions, 385 GO terms for biological processes, and 51 GO terms for cellular components (Table S2). Figure 6 shows the top 10 significantly enriched GO in the LPS-EXO and CTRL-EXO comparison. In KEGG pathway analysis, 20 KEGG pathways were related to target genes, and most of the target genes were related to the MAPK signaling pathway (Table S2 and Figure 6). Using 2,274 genes from POLY-

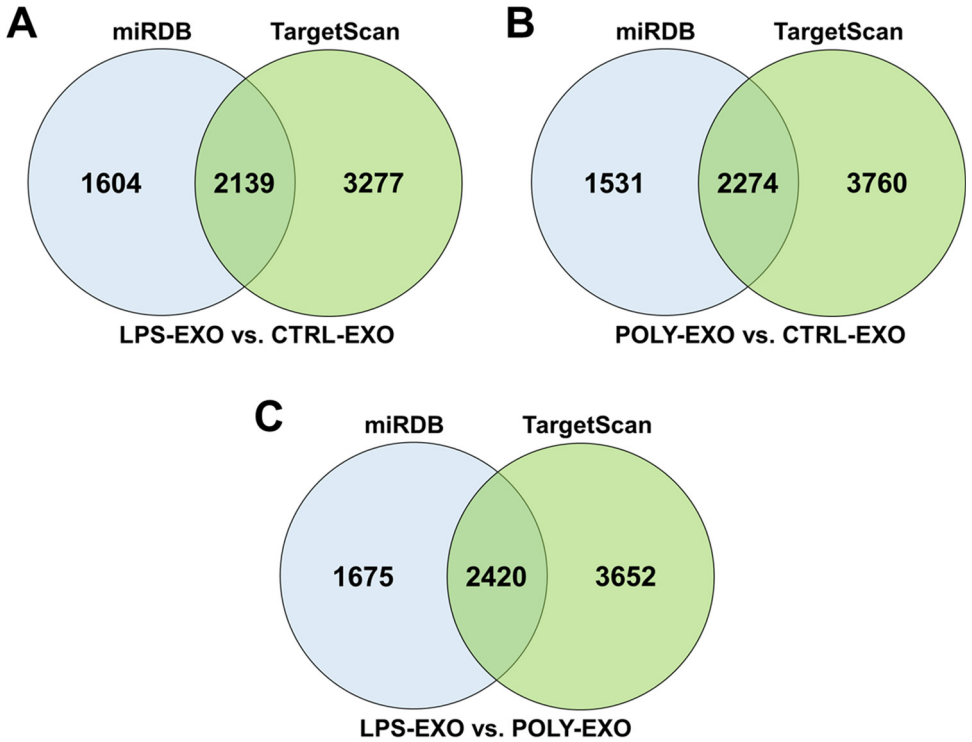

Figure 5. Venn diagram of predicted target genes from miRDB and TargetScan. Target genes of DE miRNAs from (A) lipopolysaccharide-stimulated exosomes (LPS-EXO) vs. unstimulated HD11 (CTRL-EXO), (B) poly(I:C)-stimulated exosomes (POLY-EXO) vs. CTRL-EXO, and (C) LPS-EXO vs. POLY-EXO were predicted using two different software, miRDB and TargetScan. The numbers indicate the gene counts in the indicated area.

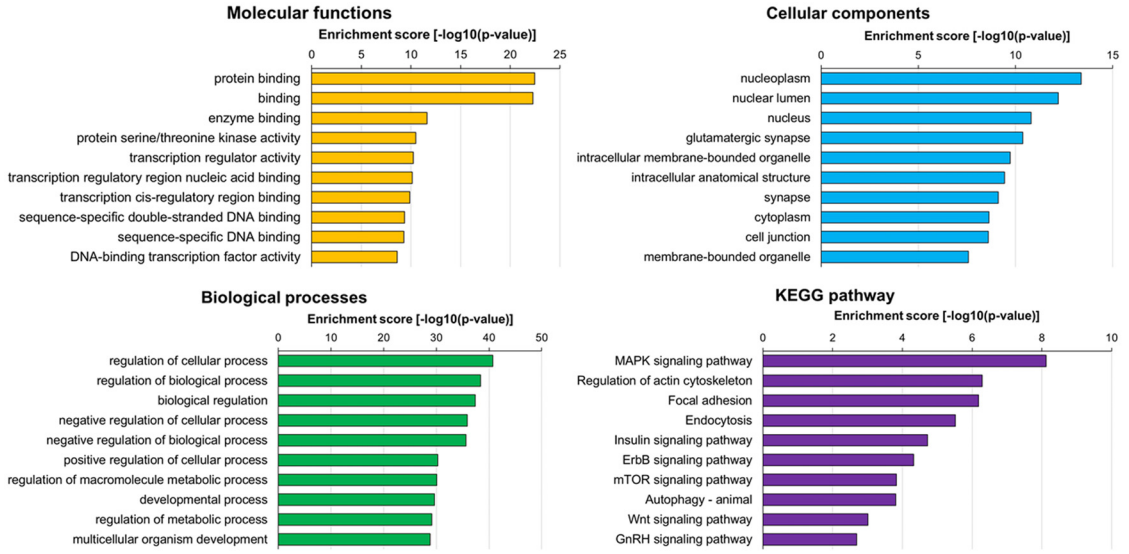

Figure 6. TOP 10 significantly enriched Gene ontology (GO) and KEGG analysis using target genes from DE miRNAs of lipopolysaccharide-stimulated exosomes (LPS-EXO) vs. unstimulated HD11 (CTRL-EXO).

EXO vs. CTRL-EXO comparison, 52 GO terms were found in molecular functions, 441 GO terms in biological processes, and 56 GO terms in cellular components (Table S3). Figure S2 also demonstrates the top 10 significantly enriched GO in POLY-EXO vs. CTRL-EXO comparison. In KEGG pathway analysis, 19 KEGG pathways were identified, and the MAPK signaling pathway was the most enriched pathway (Table S3 and Figure S2). Finally, in the LPS-EXO vs. POLY-EXO comparison, 51 GO terms in molecular functions, 534 GO terms in biological processes, and 66 GO terms in cellular components were found (Table S4). Moreover, Figure S3 reveals the top 10 significantly enriched GO in the LPS-EXO vs. POLY-EXO comparison. In KEGG pathway analysis, 19 pathways were found, and the Wnt signaling pathway was the most enriched pathway (Table S4 and Figure S3).

Validation of Sequencing Results by qRT-PCR

Small RNA sequencing of exosomes was confirmed using qRT-PCR. For qRT-PCR, 6 miRNAs were selected from the overlapping DE miRNAs in 3 comparisons. Expression levels of miRNAs were normalized using CTRL-EXO, and furthermore qRT-PCR results were consistent with sequencing results (Figure 7). The expression of gga-miR-142-3p was 0.16 times lower in LPS-EXO and 4.09 times higher in POLY-EXO, as

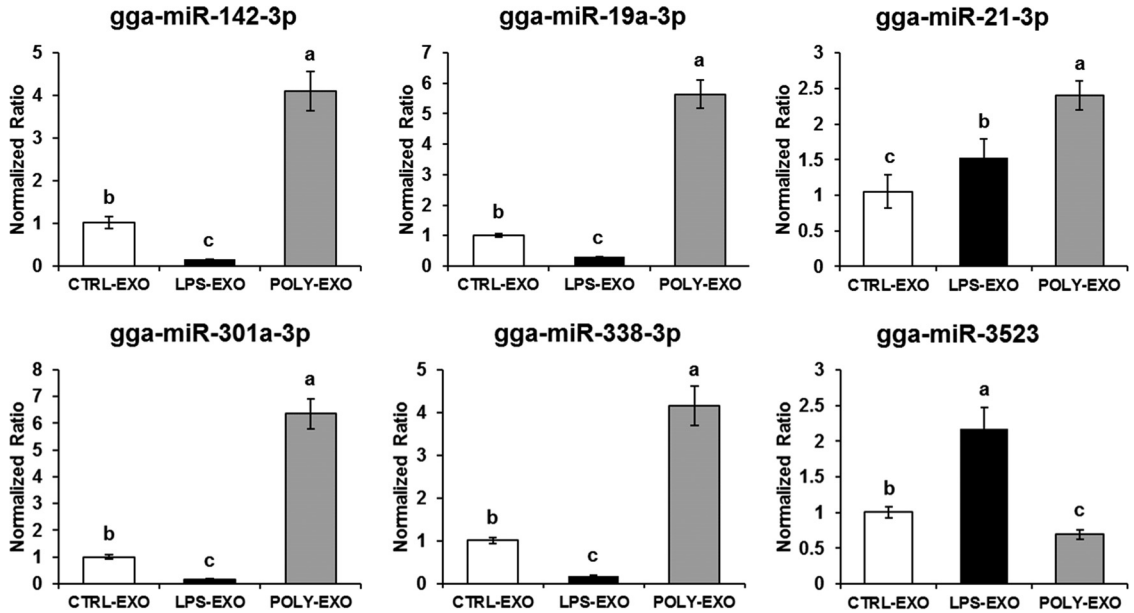

Figure 7. qRT-PCR of exosomal miRNA. Relative quantitation data are represented as mean ± SEM normalized to U1A using the $2^{-\Delta\Delta Ct}$ method. The expression level of unstimulated HD11 (CTRL-EXO) was used for normalization. The data are expressed as the mean ± standard error of the mean and are representative of three independent experiments. Different lowercase letters above the dots indicate significant differences ($P < 0.05$) as determined by analysis of variance with Tukey's multiple comparison test.

compared with CTRL-EXO. Expression patterns of gga-miR-19a-3p was 0.31-fold change in LPS-EXO and 5.63-fold change in POLY-EXO compared with CTRL-EXO. gga-miR-21-3p was 1.53-fold change in LPS-EXO and 2.41-fold change in POLY-EXO compared with CTRL-EXO. gga-miR-301a-3p was 0.17-fold change in LPS-EXO and 6.36-fold change in POLY-EXO compared with CTRL-EXO. gga-miR-338-3p was 0.17-fold change in LPS-EXO and 4.15-fold change in POLY-EXO compared with CTRL-EXO. gga-miR-3523 was 2.17 fold-change in LPS-EXO and 0.70-fold change in POLY-EXO compared with CTRL-EXO.

DISCUSSION

Exosomes are important mediators of cell communication and released exosomes from donor cells can be delivered to distant and neighboring cells by biological fluids. In particular, miRNAs delivered by exosomes can regulate gene expression in recipient cells. Moreover, our previous studies have demonstrated that exosomes from LPS and poly(I:C)-stimulated chicken macrophage cell line modulate immune responses (Hong et al., 2021a, b). Therefore, in this study, we analyzed miRNA profiles of LPS and poly(I:C)-stimulated chicken macrophage cell lines by high-throughput small RNA sequencing. miRNAs can be key regulatory factors in the various immunomodulatory roles of exosomes. For examples, the expression of exosomal miRNA from bone marrow-derived dendritic cells was different depending on their maturation, and delivered exosomal miRNAs regulate the expression of their target genes (Montecalvo et al., 2012). Moreover, exosomes derived from interferon-α and LPS-stimulated monocytes changed compositions of miRNAs and stimulated brain vascular function through the TLR4/myeloid differentiation primary response gene 88 pathway (Dalvi et al., 2017). Exosomes derived from LPS-preconditioned mesenchymal stromal cells alleviate inflammation and enhance cutaneous wound healing by delivering let-7b (Ti et al., 2015). Furthermore, exosomes derived from tumor-associated macrophages express miR-501-3p, deliver miR-501-3p, inhibit the expression of tumor suppressor TGFBR3 gene, and promote pancreatic ductal adenocarcinoma (Yin et al., 2019). Interestingly, Neerukonda et al. (2019) compared exosomal miRNA expression pattern between Marek's disease virus (**MDV**)-vaccinated chickens and unvaccinated chickens and they found that exosomes from MDV-vaccinated chickens contained MDV mRNAs that can induce immune response by delivered to antigen presenting cells.

In this study, poly(I:C) was used to stimulate the chicken macrophage cell line. Since dsRNA is generated via viral replication, stimulation of chicken macrophage cell line with poly(I:C), a synthetic dsRNA, simulates viral infection by activating TLR3 and MDA-5. In POLY-EXO vs. CTRL-EXO comparison, gga-miR-142-5p was upregulated and gga-let-7b and gga-miR-122-5p were downregulated. In a previous study, we analyzed miRNA profiles of exosomes derived from avian influenza virus H5N1-infected chickens and found that gga-miR-142-5p, gga-let-7b, and gga-miR-122-5p were differentially expressed between infected and noninfected exosomes (Hong et al., 2021c). In particular, expression patterns were similar to those in this study—gga-miR-142-5p was upregulated (2.96-fold change), and gga-let-7b (-3.43 fold-change) and gga-miR-122-5p (−2.89 fold change) were downregulated. Moreover, for DE miRNAs from LPS vs. CTRL-EXO comparison, expression patterns of gga-miR-21-3p (2.59 fold change) and gga-miR-146a-5p (4.58-fold change) were also similar to those of a previous study; mmu-miR-21-3p (114.07-fold change) and mmu-miR-146a-5p (9.81-fold change) were upregulated in exosomes derived from LPS-stimulated RAW 264.7, compared with non-stimulated cells (McDonald et al., 2014). In addition, for LPS-EXO vs. CTRL-EXO comparison, the expression level of gga-miR-29b-2-5p was the lowest (−16.77 fold change). MicorRNA-29b-5p promotes the binding of *Shigella flexneri* to host cells and replication (Sunkavalli et al., 2017). Because *Shigella flexneri* is a gram-negative bacterium, we suggest that upon stimulation by LPS, a structural component of gram-negative bacteria, macrophages downregulate the expression of gga-miR-29b-2-5p to inhibit bacterial binding and replication, and that information will be delivered to other immune cells by exosomes.

The MAPK signaling pathway plays an important role in host defense against bacterial and viral infections by regulating the inflammatory response (He et al., 2018) and Wnt signaling pathways plays various roles, such as maintaining homeostasis of immune response, immunological surveillance, and phagocytosis against infected pathogens (Jati et al., 2019). In KEGG pathway analysis, the MAPK signaling pathway was strongly regulated by target genes of DE miRNAs in the three comparisons (Figure 6 and Figures S2 and S3). Moreover, the Wnt signaling pathway was strongly related to the target genes of DE miRNAs in LPS-EXO vs. POLY-EXO. Therefore, we propose that exosomal miRNAs from LPS and poly(I:C)-stimulated chicken macrophages can regulate the MAPK and Wnt signaling pathways for antiviral immune response.

In summary, we examined the expression of exosomal miRNAs of LPS and poly(I:C)-stimulated chicken macrophage cell lines by small RNA sequencing. A total of 36 DE miRNAs were found in LPS-EXO vs. CTRL-EXO, 42 DE miRNAs in POLY-EXO vs. CTRL-EXO, and 45 DE miRNAs in LPS-EXO vs. POLY-EXO. Moreover, we predicted target genes of DE miRNAs using miRDB and TargetScan. Interestingly, MAPK and Wnt signaling pathways were highly correlated with DE miRNAs in 3 comparisons. This study provides an understanding of the immuno-regulatory mechanisms of exosomal miRNAs against bacterial and viral infections.

ACKNOWLEDGMENTS

This research was funded by a grant (NRF-2021R1A2C2005236) from the National Research Foundation of the Republic of Korea.

DISCLOSURES

The authors declare that they have no competing interests.

SUPPLEMENTARY MATERIALS

Supplementary material associated with this article can be found, in the online version, at doi:10.1016/j.psj.2022.102141.

REFERENCES

Aderem, A., and D. M. Underhill. 1999. Mechanisms of phagocytosis in macrophages. Annu. Rev. Immunol. 17:593–623.

Billack, B. 2006. Macrophage activation: role of toll-like receptors, nitric oxide, and nuclear factor kappa B. Am. J. Pharm. Educ. 70:102.

Boulanger, C. M., X. Loyer, P.-E. Rautou, and N. Amabile. 2017. Extracellular vesicles in coronary artery disease. Nat. Rev. Cardiol. 14:259.

Chen, Y., G. Li, and M.-L. Liu. 2018. Microvesicles as emerging biomarkers and therapeutic targets in cardiometabolic diseases. Genomics Proteomics Bioinform. 16:50–62.

Dalvi, P., B. Sun, N. Tang, and L. Pulliam. 2017. Immune activated monocyte exosomes alter microRNAs in brain endothelial cells and initiate an inflammatory response through the TLR4/MyD88 pathway. Sci. Rep. 7:1–12.

Gross, J. C., V. Chaudhary, K. Bartscherer, and M. Boutros. 2012. Active Wnt proteins are secreted on exosomes. Nat. Cell Biol. 14:1036.

He, Y., W. Yao, P. Liu, J. Li, and Q. Wang. 2018. Expression profiles of the p38 MAPK signaling pathway from Chinese shrimp Fenneropenaeus chinensis in response to viral and bacterial infections. Gene 642:381–388.

Hong, Y., J. Lee, T. H. Vu, S. Lee, H. S. Lillehoj, and Y. H. Hong. 2020. Immunomodulatory effects of avian β-defensin 5 in chicken macrophage cell line. Res. Vet. Sci. 132:81–87.

Hong, Y., J. Lee, T. H. Vu, S. Lee, H. S. Lillehoj, and Y. H. Hong. 2021a. Exosomes of lipopolysaccharide-stimulated chicken macrophages modulate immune response through the MyD88/NF-κB signaling pathway. Dev. Comp. Immunol. 115:103908.

Hong, Y., J. Lee, T. H. Vu, S. Lee, H. S. Lillehoj, and Y. H. Hong. 2021b. Immunomodulatory effects of poly (I: C)-stimulated exosomes derived from chicken macrophages. Poult. Sci. 100:101247.

Hong, Y., A. D. Truong, J. Lee, T. H. Vu, S. Lee, K.-D. Song, H. S. Lillehoj, and Y. H. Hong. 2021c. Exosomal miRNA profiling from H5N1 avian influenza virus-infected chickens. Vet. Res. 52:1–11.

Jati, S., T. R. Sarraf, D. Naskar, and M. Sen. 2019. Wnt signaling: pathogen incursion and immune defense. Front. Immunol. 10:2551.

Kalluri, R., and V. S. LeBleu. 2020. The biology, function, and biomedical applications of exosomes. Science 367:6478.

Kim, T. H., and H. Zhou. 2015. Functional analysis of chicken IRF7 in response to dsRNA analog poly (I: C) by integrating overexpression and knockdown. PLoS One 10:e0133450.

Klasing, K. C., and R. K. Peng. 1987. Influence of cell sources, stimulating agents, and incubation conditions on release of interleukin-1 from chicken macrophages. Dev. Comp. Immunol. 11:385–394.

Koh, T. J., and L. A. DiPietro. 2011. Inflammation and wound healing: the role of the macrophage. Expert Rev. Mol. Med. 13:e23.

Livak, K. J., and T. D. Schmittgen. 2001. Analysis of relative gene expression data using real-time quantitative PCR and the $2^{-\Delta\Delta CT}$ method. Methods 25:402–408.

Mathivanan, S., H. Ji, and R. J. Simpson. 2010. Exosomes: extracellular organelles important in intercellular communication. J. Proteom. 73:1907–1920.

McDonald, M. K., Y. Tian, R. A. Qureshi, M. Gormley, A. Ertel, R. Gao, E. A. Lopez, G. M. Alexander, A. Sacan, and P. Fortina. 2014. Functional significance of macrophage-derived exosomes in inflammation and pain. Pain 155:1527–1539.

Montecalvo, A., A. T. Larregina, W. J. Shufesky, D. Beer Stolz, M. L. Sullivan, J. M. Karlsson, C. J. Baty, G. A. Gibson, G. Erdos, and Z. J. B. Wang. 2012. Mechanism of transfer of functional microRNAs between mouse dendritic cells via exosomes. Am. J. Hematol. 119:756–766.

Neerukonda, S. N., P. Tavlarides-Hontz, F. McCarthy, K. Pendarvis, and M. S. Parcells. 2019. Comparison of the transcriptomes and proteomes of serum exosomes from Marek's disease virus-vaccinated and protected and lymphoma-bearing chickens. Genes 10:116.

Reimer, T., M. Brcic, M. Schweizer, and T. W. Jungi. 2008. poly (I: C) and LPS induce distinct IRF3 and NF-κB signaling during type-I IFN and TNF responses in human macrophages. J. Leukoc. Biol. 83:1249–1257.

Sunkavalli, U., C. Aguilar, R. J. Silva, M. Sharan, A. R. Cruz, C. Tawk, C. Maudet, M. Mano, and A. Eulalio. 2017. Analysis of host microRNA function uncovers a role for miR-29b-2-5p in Shigella capture by filopodia. PLoS Pathog 13:e1006327.

Thompson, M. R., J. J. Kaminski, E. A. Kurt-Jones, and K. A. Fitzgerald. 2011. Pattern recognition receptors and the innate immune response to viral infection. Viruses 3:920–940.

Ti, D., H. Hao, C. Tong, J. Liu, L. Dong, J. Zheng, Y. Zhao, H. Liu, X. Fu, and W. Han. 2015. LPS-preconditioned mesenchymal stromal cells modify macrophage polarization for resolution of chronic inflammation via exosome-shuttled let-7b. J. Transl. Med. 13:308.

Tkach, M., and C. Théry. 2016. Communication by extracellular vesicles: where we are and where we need to go. Cell 164:1226–1232.

Yin, Z., T. Ma, B. Huang, L. Lin, Y. Zhou, J. Yan, Y. Zou, and S. Chen. 2019. Macrophage-derived exosomal microRNA-501-3p promotes progression of pancreatic ductal adenocarcinoma through the TGFBR3-mediated TGF-β signaling pathway. J. Exp. Clin. Cancer Res. 38:310.

Zhang, J., S. Li, L. Li, M. Li, C. Guo, J. Yao, and S. Mi. 2015. Exosome and exosomal microRNA: trafficking, sorting, and function. Genomics Proteomics Bioinform. 13:17–24.